

Resistivity of $\text{Ni}_x\text{Cu}_{1-x}$ Alloy Films

M. K. Loudjani^{1,*} and C. Sella².

¹ Université Paris sud, ICMO-UMR 8182 (CNRS), SP2M-Bâtiment 410, 91405 Orsay Cedex, France.

² Institut des Nano-Sciences de Paris, Université de Paris-VI, campus Bouicaut, 140 rue de Lourmel 75015 Paris, France.

Received: 8 Sep. 2015, Revised: 2 Oct. 2015, Accepted: 10 Oct. 2015.

Published online: 1 Jan. 2016.

Abstract: In this study we compare the influence of chemical composition and microstructural defects on the resistivity of $\text{Ni}_x\text{Cu}_{1-x}$ film alloys. The relative variation of the resistivity of $\text{Ni}_x\text{Cu}_{1-x}$ bulk alloy by nickel atom substituted is the same than that in a $\text{Ni}_x\text{Cu}_{1-x}$ alloy film. When the density of randomly distributed defects increases, with an average distance between electronic scattering centers comparable to the mean free path of electrons at the Fermi level, the resistivity reaches its maximum. Near the ambient temperature the maximum of resistivity of $\text{Ni}_x\text{Cu}_{1-x}$ alloy films is obtained for an atomic composition of nickel equal to 60 %. Near the ambient temperature the minimum of the temperature coefficient of resistivity in $\text{Ni}_x\text{Cu}_{1-x}$ alloy films is obtained for an atomic composition (46 ± 2)% of nickel.

Keywords: $\text{Ni}_x\text{Cu}_{1-x}$ film alloys resistivity, Gradient-microstructure-chemical composition-Resistivity, temperature coefficient of resistivity, $\text{Ni}_x\text{Cu}_{1-x}$ metastable phase transition.

1 Introduction

A large amount of work has been performed on the transport and magnetic properties on $\text{Ni}_x\text{Cu}_{1-x}$ bulk alloys in relation with their electronic structure. Among the first theoretical studies and models which takes into account the effects of the chemical composition one can quote the review article of N. F. Mott [1]. The studies of the fluctuation of local composition in binary alloy on the resistivity and that concerning the local concentration of electrons on temperature coefficient of electrical resistivity was approached by R. Smoluchowski, [2] and recently described by V.F. Gantmakher [3]. In the case of metal thin films with column-like grains the expression of the resistivity according to the models developed respectively by K. Fuchs- E.H.Sondheimer [4,5] and by F. Mayadas- M. Shatzkes [6], depends on the thickness of films, the conduction electron mean free path, the mean grain size and electron scattering on the surface of films and on the grain boundaries. In this work we investigated the transport properties of $\text{Ni}_x\text{Cu}_{1-x}$ film alloys in order to elucidate the correlation between the various classes of defects (chemical composition, grain boundaries, and interfaces) and thin film resistivity. The resistivity measurement method by 4-points probes in-line was used to analyze these effects. The samples studied in this work are $\text{Ni}_x\text{Cu}_{1-x}$ thin alloy films obtained by RF sputtering and deposited on two types of substrates of different surface roughness: glass substrates and polycrystalline α -alumina substrates. The atomic

composition of nickel in $\text{Ni}_x\text{Cu}_{1-x}$ film alloys varies in the range $1.5\% < x < 81\%$. The $\text{Ni}_x\text{Cu}_{1-x}$ solid solutions present distances between sources of electron scattering comparable with the mean free path of the electrons with energy close to the Fermi level whereas the average distance between defects (grains boundary, interfaces) is comparable with the mean free path of the conduction electrons. In order to specify the contribution of the various classes of defects (chemical composition, grains size) on the electric properties of films, annealing under vacuum was performed. $\text{Ni}_x\text{Cu}_{1-x}$ bulk alloys, and Ni/Cu bilayers films having the same nickel average composition as the $\text{Ni}_x\text{Cu}_{1-x}$ film alloys were taken as reference samples. The maximum of the resistivity of $\text{Ni}_x\text{Cu}_{1-x}$ film alloys is obtained for an atomic composition of nickel near to 60%. Measurements of the temperature coefficient of resistivity, carried out around the ambient temperature, presents a minimum for an atomic composition of nickel close to 46%. In addition to the chemical disorder created by the effect of alloying and the effect of the chemical composition on the microstructure, the $\text{Ni}_x\text{Cu}_{1-x}$ alloys exhibit a ferromagnetic to nonmagnetic transition [7,8] at a temperature close to the ambient temperature.

A specific experimental device and adapted instrumentation was developed to study electrical measurements on thin films, under vacuum and at controlled temperature. Combination of various techniques: Energy-Dispersive X-ray Spectrometry (E.X.D.S), X-rays diffractions, Transmission Electronic Microscopy (T.E.M)

*Corresponding author E-mail: mohamed-khireddine.loudjani@u-psud.fr

on thin films were associated to electrical resistivity measurements.

2 Elaboration of $\text{Ni}_x\text{Cu}_{1-x}$ Alloy Films with Chemical Composition Gradient

We choose the technique of cosputtering of continuous compositional ranges for two components system introduced by J.J. Hanak [9, 10], Fig.1. The theoretical principle of the method of co-pulverization deduced from the law of Kundsén [11] applied to evaporation is exposed in work of Gnaedinger [12] and G.C. Schwartz [13].

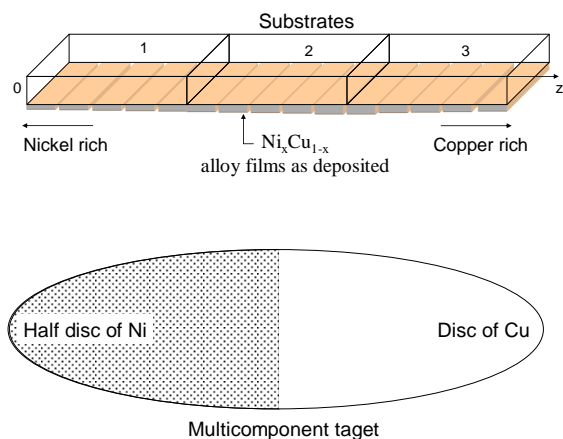


Fig.1: Experimental device used to prepare $\text{Ni}_x\text{Cu}_{1-x}$ alloy films in case of target for strong gradient.

The technique consists in co-sputtering $\text{Ni}_x\text{Cu}_{1-x}$ alloy films from a target made of nickel and copper. Fig.-5a-5b, represent the two geometries chosen to obtain the development of the two gradients of compositions of $\text{Ni}_x\text{Cu}_{1-x}$ film alloys. In a first case the target consists of a copper disc partially covered by a half disc of nickel, Fig.5a, and in the second case the copper disc target is covered by a nickel sector Fig.5b representing 18% of the surface of the copper disc. The thin films were prepared by R.F. sputtering using a diode module having a power supply operating at 13.5 MHz, a disk-shaped cathode of diameter 13 cm and a target to substrate distance of 4 cm. The base pressure of the vacuum chamber was $1.33 \cdot 10^{-4}$ Pa and sputtering was performed in an argon atmosphere at a pressure of 1.33 Pa. Before deposition we operate a presputtering of the target to eliminate the impurity gases present at the surface of the cathode. During this presputtering time (15 to 30 mn) the substrate is protected by a shutter. The deposit ion rate varies from that of copper film (about $3.54 \text{ \AA} \cdot \text{s}^{-1}$) to that of nickel films (about $1.94 \text{ \AA} \cdot \text{s}^{-1}$).

3 Substrates

Two types of substrates are used:

- 1737 corning glass in one hand: because of its thermo-mechanical properties adapted to metal films deposited and of a good surface quality, allow to make local thickness measurements. In order to prepare a large range of composition in each cosputtering run, three square substrates of 35 mm side and 1 mm thickness, juxtaposed are used as shown in Fig. 2. Before each deposit a periodic network of parallel strips of 0.7 mm width, distant of 6.5 mm, is drawn with a felt pen, on the surface of each substrate.

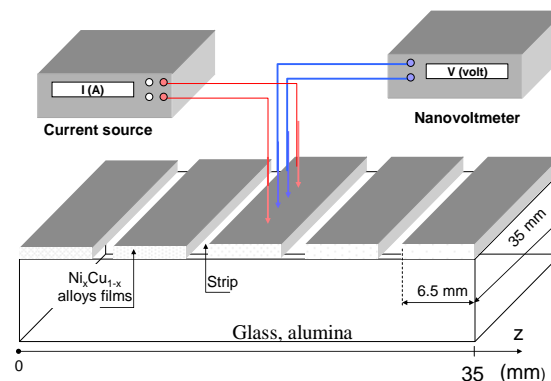


Fig.2: Geometrical shape of $\text{Ni}_x\text{Cu}_{1-x}$ alloy films samples deposited on substrates (glass, alumina). Principle of resistance measurement.

This strips allows after dissolution with acetone (lift off technique) and to delimitate separated rectangular (6.5x35 mm) film samples. The steps obtained are used for local thicknesses measurements.

- Polycrystalline α -alumina substrates having an average size of grains $G = 5 \pm 4 \text{ \mu m}$, Fig.3. Two rectangular sheets of 50 mm length, 35 mm width, and 1 mm thickness are used for each deposit. Rectangular samples of the same shape than previously described and separated by insulating tracks are located on each of the two alumina plates.

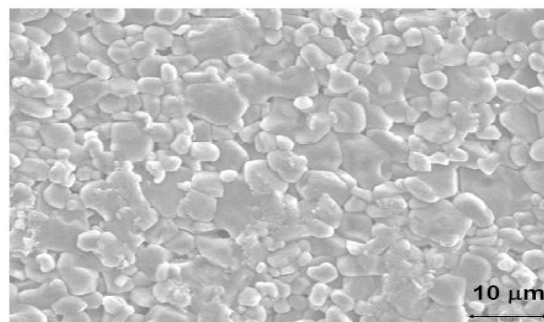


Fig.3: Surface topography of a $\text{Ni}_8\text{Cu}_{92}$ film alloy deposited on a α -alumina substrate.

In addition to the chemical difference between the two substrates, the roughness of two surfaces vary from 5 nm for the Corning glass substrates to about 510^3 nm for the α -alumina substrates.

4 Annealing of Ni_xCu_{1-x} Film Alloy

The annealing aims to increase the average grain size and to lower the rate of defects during the grain growth. The heating, during 90 mn, up to the temperature of 465°C, and the cooling of the samples to ambient temperature are carried out in secondary vacuum. The rise in temperature from the ambient temperature to 465°C is approximately 1.5 hour whereas the decrease to the ambient temperature is 3.5 hours.

5 Thickness Measurements of Ni_xCu_{1-x} Film Alloys

Thickness measurements are carried out on each step separating two bands using an optical phase shift interferometric microscope. The average thicknesses of Ni_xCu_{1-x} films varies between 80 nm and 215 nm. The profiles of thicknesses determined for the two limits of composition gradient are reported in figures Fig.4a, Fig.4b. Each profile thickness is fitted using two curves of "Gaussian" distribution.

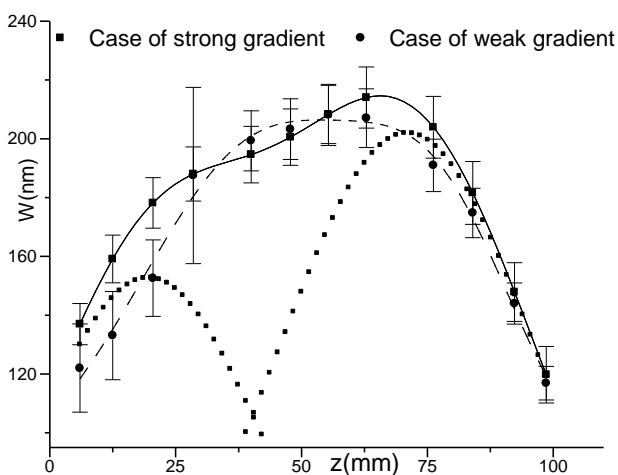
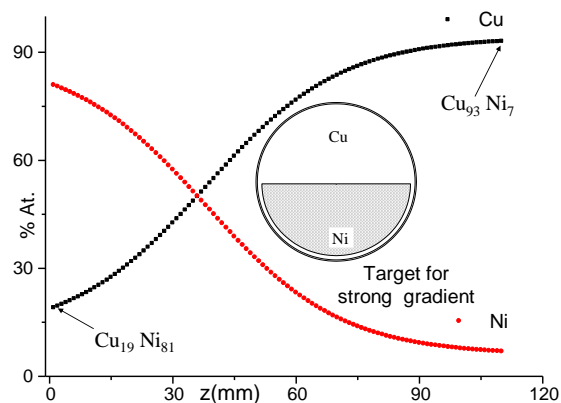


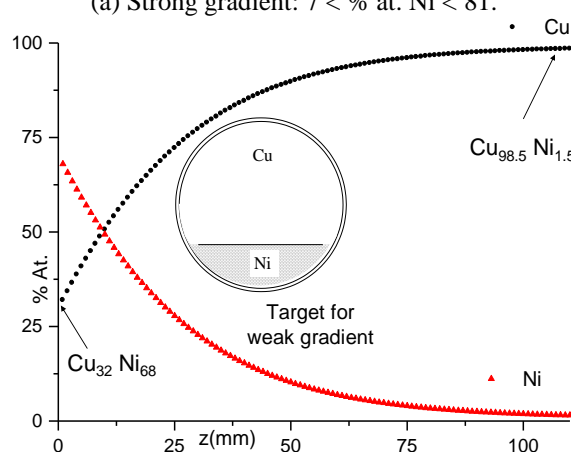
Fig.4: Thicknesses profile curves of Ni_xCu_{1-x} alloy films deposited on glass substrates and obtained for two gradient of composition.

6 Chemical Analyses of the Composition Gradient Ni_xCu_{1-x} Film Alloys

The chemical profiles of nickel and copper compositions along the direction of the gradient are obtained on MEB-Leica equipped with an X-ray detector from Röntech Company. The kinetic energy of the primary electrons used for the chemical analysis is of 15 keV. The concentrations of nickel and copper, obtained from the intensities of K_{α-Ni} and K_{α-Cu} emission lines, are carried out along the axis of each rectangular band with an average step of 2 mm. From the apparent experimental concentrations (C_{Ni})_{exp}, (C_{Cu})_{exp}, we calculated the real concentrations (C_{Ni})_F and (C_{Cu})_F of the chemical elements in Ni_xCu_{1-x} thin films.



(a) Strong gradient: 7 < % at. Ni < 81.



(b) Weak gradient: 1.5 < % at. Ni < 68.

Fig.5: Nickel and copper concentration gradient in Ni_xCu_{1-x} alloys films for two geometrical configurations of the multicomponent targets.

The standard samples used for this quantitative analysis are Ni/Cu bilayered films. The mean atomic composition of nickel and copper in the Ni/Cu bilayered films is calculated according to equation (1):

$$(C_{Ni})_F = \frac{w_{Ni} a_{Cu}^2}{w_{Ni} a_{Cu}^2 + w_{Cu} a_{Ni}^2} \tag{1}$$

where a_{Ni} and a_{Cu} are the cubic cells parameters of nickel and copper layers and w_{Ni}, w_{Cu} are respectively the thicknesses of these two layers. The total thickness of Ni/Cu bilayered films was intended to be equal to that of the Ni_xCu_{1-x} film alloy. This method enabled us to check the conservation of the ratio of the concentrations in the Ni/Cu bilayered films:

$$\frac{(C_{Ni})_F}{(C_{Cu})_F} = \frac{(C_{Ni})_{exp}}{(C_{Cu})_{exp}} \tag{2}$$

By combining equation-2, and the equation (3) expressing the mass law conservation:

$(C_{Ni})_F + (C_{Cu})_F = 1 \leq (3)$, we deduced the local concentration of nickel (C_{Ni})_F and copper (C_{Cu})_F in Ni_xCu_{1-x} film alloys. The results of chemical analyzes relating to the two limits of composition are given in the figures Fig.5a-5b. In the configuration with strong gradient, the atomic fraction of nickel varies between $7\% < x < 81\%$, Fig.5a, whereas in the second configuration with weak gradient the nickel concentration varies between $1.5\% < x < 68\%$, Fig.5b.

7 Morphology and Microstructure of the Ni_xCu_{1-x} Film Alloys

Two techniques were used to characterize the microstructure of films: transmission electronic microscopy (TEM) and X-ray diffraction.

7.1 Microstructural analysis of the Ni_xCu_{1-x} alloys by T.E.M.

The microstructure of the films was studied by T.E.M. on samples deposited on to carbon films supported by a fine copper mesh. The evolution of the microstructure of the samples according to the composition of alloy films and the law of variation of the average grains size of alloys are reported in figure Fig.6.

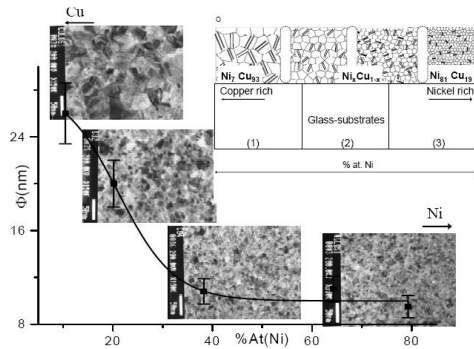


Fig. 6: Variation of the mean grain size of Ni_xCu_{1-x} alloys films, according to the atomic composition of nickel.

The average grain size determined on as deposited films varies from a mean size of $\phi = 8 \pm 3$ nm for samples with a high nickel concentration (% At.-Ni = 81), up to a mean size equal of $\phi = 30 \pm 10$ nm for samples with a high copper concentration (% At.-Cu = 94 %).

7.2 Structural analysis of Ni_xCu_{1-x} alloy films by X-ray diffraction:

The analyses are carried out on a Philips generator-X equipped with a copper anticathode. A focused beam of average size 1*3 mm was used to obtain the diffraction spectra of the films in the direction of the gradient. Variation of the position of the diffraction peak (111) angle along the x-axis was measured at ambient temperature from

the area with high nickel concentration up to the area with high copper concentration. The average step between two points of spectral analyzes is of approximately of 2.5 mm.

The variation of the cubic cell parameters according to the composition of Ni_xCu_{1-x} alloy, was deduced for the two gradients composition. Figure-7 shows that the curve is not linear contrary to the Vegard law, applicable to an equilibrium solid solution.

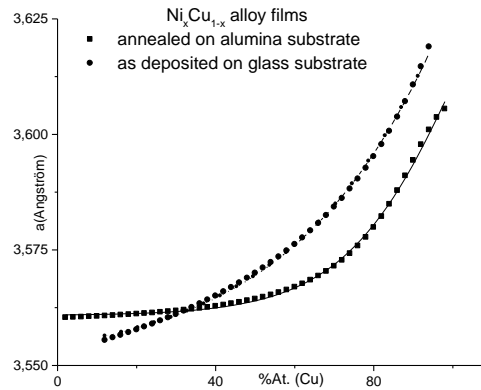


Fig.7: Cubic cell parameter variation according to the content of copper in Ni_xCu_{1-x} alloy films as deposited and after annealing.

This difference is due to the importance of the bulk fraction of the grain boundaries present in film. The grain boundaries behave as a second phase whose proportion grows when the size of grains decreases. An order of magnitude of this fraction is calculated, in the case of column-like grains with square section, starting from the

relation: $2\% < f \approx \frac{3\delta}{\phi} < 20\%$, where ϕ the mean grain

size and $\delta \cong 0.5$ nm is the mean width of the grain boundary.

8 Resistivity of Ni_xCu_{1-x} Alloy Films

8.1 Influence of the composition gradient on the resistivity of Ni_xCu_{1-x} alloy films

The resistance measurements are taken while locating the four probes points in the middle of each rectangular band, in the direction length and parallel to the two sides of the band, Fig.2. The calculation of the resistivity is deduced from the measured resistances by using the models developed by Smits [14]. The variations of the resistivity as a function of the position on the substrates and as a function to the atomic composition of nickel are reported respectively in the figures Fig.8 and Fig.9. On Ni_xCu_{1-x} as deposited films, the resistivity of the samples with weak gradient, $1.5\% < x < 68\%$, decreases in a continuous way since the areas of the samples presenting a high nickel concentration up to the areas with high copper

concentration, whereas in the case of the samples with strong gradient, $7\% < x < 85\%$, the resistivity presents a maximum.

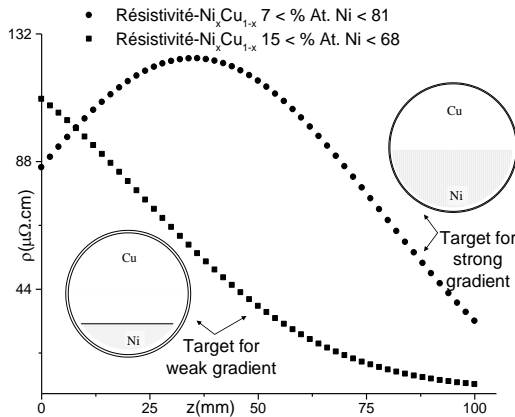


Fig.8: Variation of the resistivity of Ni_xCu_{1-x} alloy films along the x-axis for the two gradients of composition.

In this case the maximum of resistivity in Ni_xCu_{1-x} alloy films is obtained for an atomic composition of nickel equal to $60 \pm 1\%$, Fig-9.

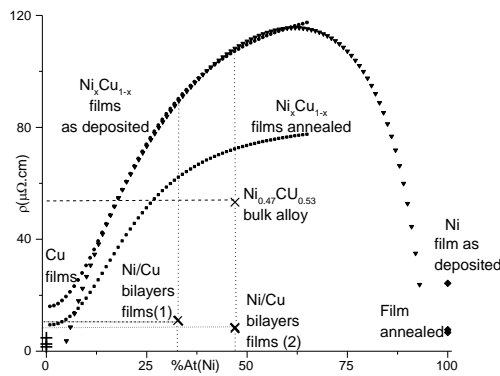


Fig.9: Variation of the resistivity according to the nickel content in Ni_xCu_{1-x} alloy films for the two targets and influence of annealing. Resistivity of Ni_xCu_{1-x} alloy films compared to the Ni_xCu_{1-x} bulk alloy and Ni/Cu bilayers films [16].

The fitting law describing the variation of the resistivity as a function of the atomic fraction in film alloys is a polynomial of degree five. This variation of the resistivity of the Ni_xCu_{1-x} alloy films differs from the parabolic law according to Nordheim's model: $\rho = \rho_0 + C*x*(1-x)$, established if electronic transport in bulk alloys is controlled by electron transitions from "ns" to the "ns" band and which gives a maximum of resistivity for an atomic fraction equal to $x = 50\%$, where ρ_0 is the resistivity of the solvent (Cu) and C a constant. In this last case the composition, independently of the electronic structure, corresponds to that of an alloy presenting a random distribution of the nickel atoms and the maximum disorder.

8.2 Effect of the substrate and thermal annealing on the resistivity of Ni_xCu_{1-x} alloy films

8.2.1 Resistivity of Ni_xCu_{1-x} alloy films in case of a strong nickel gradient composition

In the case of samples with strong gradient, we observe after annealing a peeling of the film. The surface peeled grows with the nickel concentration, Fig.10.

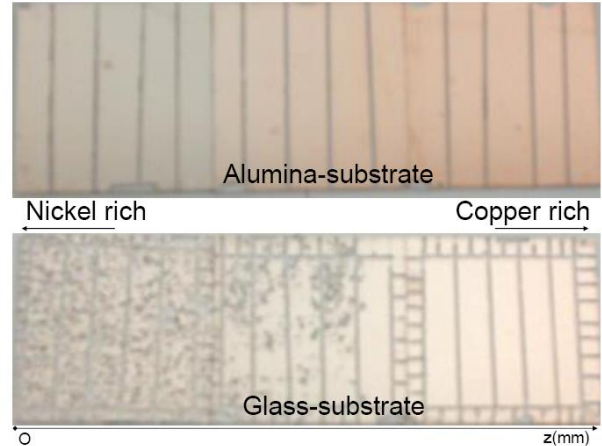


Fig.10: Peeling of Ni_xCu_{1-x} alloy films on glass during cooling in the region with high nickel content (case of strong concentration gradient).

The most important decohesions are observed for an average nickel composition $> 38\%$. This value corresponds to the threshold of nickel composition in the alloy from which the transformation of solid solution in metastable phases occurs at a temperature equal to 200°C : $\alpha \rightarrow \alpha_1 + \alpha_2$. This transformation occurring by the equilibrium diagram when the nickel concentration varies in the interval: $32 < \% \text{ At.}(\text{Ni}) < 98$ does not seem to produce a class of defects resulting in important variations of the resistivity. In addition to this phase transformation, in the area of Ni_xCu_{1-x} film alloys with strong nickel concentrations the rate of stress growth during annealing is the highest. Indeed stresses generated by the variation of the volumic fraction of the grain boundaries during the annealing of films, [15] increases with the nickel content. The average stresses growth in the Ni_xCu_{1-x} film alloys are given by the relation: $0 \leq$

$$\sigma = \frac{E(x)}{1-\nu(x)} \delta \left(\frac{1}{\phi_0(x)} - \frac{1}{\phi(x)} \right) \leq 2.3 \text{ GPa, with } 125 \leq$$

$E(x) \leq 238 \text{ GPa}$ the Young modulus of the Ni_xCu_{1-x} alloy, $0.31 \leq \nu(x) \leq 0.34$ the Poisson's ratio, $\delta \approx 0.5 \text{ nm}$ the average width of the grain boundaries, $\phi_0(x)$ the average grains size of films as deposited and $\phi(x)$ the size of the grains after annealing [16]. Films with high copper concentration present less peeling and their resistivity after annealing decreases by approximately 20%.

8.2.2 Resistivity of Ni_xCu_{1-x} film alloys with weak gradient composition

In the case of samples with weak composition gradient, peeling of films after annealing is negligible even for compositions of nickel larger than 38% atomic. After annealing the resistivity decreases by approximately 40% for the area with a high copper concentration and only 36% for the area with a high nickel concentration as shown in Fig.11a-11b. On the alumina substrates we observe a weaker peeling film during cooling.

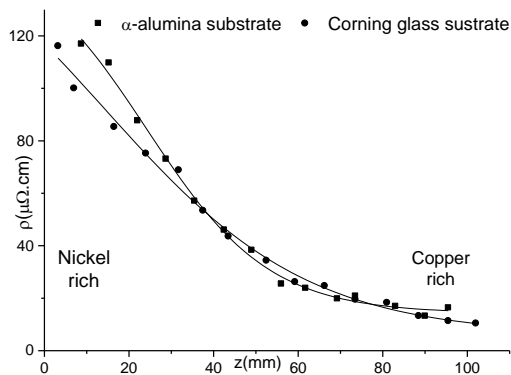


Fig.11a: Influence of the substrate on the resistivity of Ni_xCu_{1-x} alloy films as deposited.

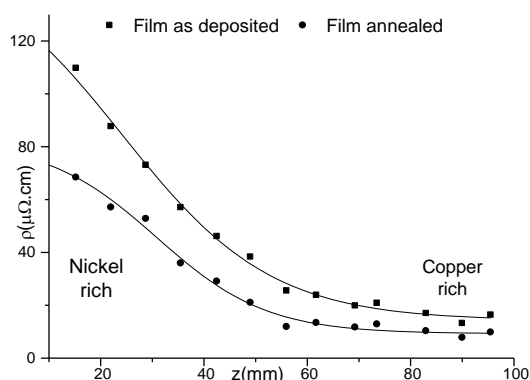


Fig.11b: Effect of the annealing on the resistivity of Ni_xCu_{1-x} alloy films deposited on α-alumina substrate.

The comparison of the films resistivity deposited on the two types of substrates shows that contrary to annealing, the topography of the alumina surface as well as the nature of the substrate have little effect on the resistivity of Ni_xCu_{1-x} film alloys. Indeed if we take as reference length the conduction electron mean free path in the Ni_xCu_{1-x} alloys calculated according to Drude model [3, 16,17]: $\lambda < 41$ nm, the micrometric scale of surface topography of the alumina substrate does not constitute a class of defects being able to affect in an important way the electronic transport in the case of Ni_xCu_{1-x} film alloys. The interface between the Ni_xCu_{1-x} film alloys and substrates after thermal annealing do not seem to undergo physico-chemical modifications on length scales of distances being able to influence the electric properties of Ni_xCu_{1-x} film alloys.

9 Temperature Coefficient of Resistivity of the Ni_xCu_{1-x} Film Alloys

The variation of the temperature coefficient resistivity was obtained on Ni_xCu_{1-x} film alloys (1.5% < x < 81%) in the temperature range 18°C < T < 40°C and vacuum (P = 1.33 Pa). The temperature coefficient decreases with the nickel concentration and as the chemical disorder increases. The minimum coefficient is obtained for an atomic nickel composition of 46%, Fig.12a.

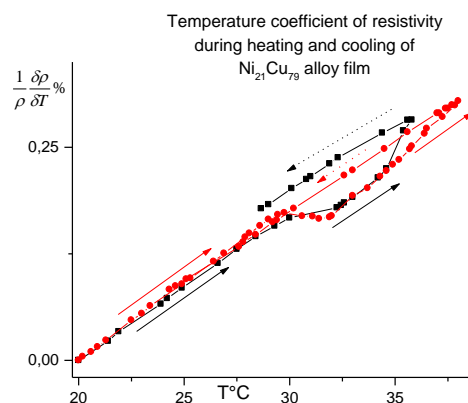


Fig.12a: Variation of the temperature coefficient of resistivity, during heating and cooling, near the ambient temperature in Ni₂₁Cu₇₉ alloy films.

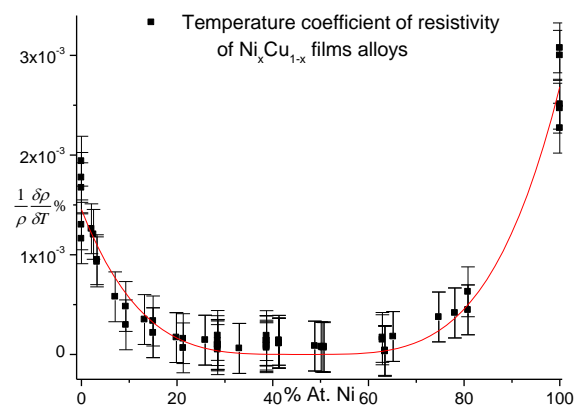


Fig.12b: Variation of the temperature coefficient of resistivity according to the nickel content in Ni_xCu_{1-x} alloy films.

For the film alloys with nickel composition lower than 20% the resistivity $\rho(T)$ varies linearly with the temperature. On the other hand for the Ni_xCu_{1-x} alloys with composition of nickel higher than 20% , Fig.12a, anomalies during the heating are observed on the curves $\rho(T)$, starting from a temperature of 29°C, Fig.12b. The temperatures at which these transitions are observed are shifted towards the high temperatures as the nickel content increases. This threshold of composition corresponds to the beginning of the metastable phase transition: $\alpha \rightarrow \alpha_1 + \alpha_2$.

10 Conclusion and Discussion

The resistivity of $\text{Ni}_x\text{Cu}_{1-x}$ film alloys increases with the nickel concentration and with the reduction of the grains size of films and thickness. By comparison the resistivity of the $\text{Ni}_{47}\text{Cu}_{53}$ film alloy with thickness $w = 204$ nm, and an average size of grains equal to 10 nm is approximately a factor of two larger than the resistivity of a bulk alloy sample of the same composition and having a thickness of 20 μm and grain size of approximately 47 nm. The resistivity of $\text{Ni}_{47}\text{Cu}_{53}$ film is more than one order of magnitude higher than the resistivity of Ni/Cu bilayers with equivalent mean atomic composition and with the same total thickness [16]. In the case of bulk annealed sample the increase of the resistivity of $\text{Ni}_{47}\text{Cu}_{53}$ alloy is 31 times larger than in the case of copper. The resistivity of $\text{Ni}_{47}\text{Cu}_{53}$ film alloys is 30 times larger than that of pure copper film. The variation of the resistivity of bulk solid solution of $\text{Ni}_x\text{Cu}_{1-x}$ by nickel atom substituted is the same that the variation of the resistivity of a $\text{Ni}_x\text{Cu}_{1-x}$ alloy film.

In the lattice of the $\text{Ni}_x\text{Cu}_{1-x}$ film alloys, the nickel introduces chemical point defects located at short distances. The average distance between nickel atoms in these films varies between 0.25 nm and 0.55 nm, these distances are much smaller than the mean free path of the conduction electrons of pure copper or nickel [16] but close to the wavelength associated with the electrons of energy close to the Fermi level. The parameters which control the resistivity of films of $\text{Ni}_x\text{Cu}_{1-x}$ are thus by order of decreasing importance, the average composition of the alloy, the average size of the grains and finally the surface contribution.

Near the ambient temperature, the maximum of resistivity in $\text{Ni}_x\text{Cu}_{1-x}$ film alloys is obtained for an atomic composition of nickel equal to 60% whereas the position of the maximum given in the literature for the bulk alloys near zero degrees is obtained by Svenson [7] at 50%. The phase transformation $\alpha \rightarrow \alpha_1 + \alpha_2$ does not seem to produce a class of defects being able to involve, at room temperature, important variations of the resistivity however the interfaces created by this demixion causes a drop in the temperature coefficient. Near the room temperature, the minimum of the temperature coefficient in $\text{Ni}_x\text{Cu}_{1-x}$ film alloys is obtained for a composition of nickel equal to 46% atomic.

Finally, through this study, let us note the interest of the technique of cosputtering for the facility of preparation and the development of new applications of thin film alloys.

Acknowledgements

The authors wish to acknowledge the staff of the Department M.P-IUT-Orsay, of ICMMO, of AIS (Université-Paris-Sud-11-Orsay), INSP -Boucicaut-Paris-VI and CECM-Vitry (CNRS) who contributed to various stages of this study.

References

- [1] N. F. Mott, Proc. Phys. Soc. 47, 571-588, (1935).
- [2] R. Smoluchowski, Phys. Rev Vol. 84, N°3, 511-518, (1951).
- [3] V.F. Gantmakher, Electrons and Disorder in Solids Clarendon Press Oxford 2005.
- [4] Fuchs, K., 1938, Proc. Camb. Phil., Soc., 34, 100.
- [5] E.H. Sondheimer, Advances in physics Vol.1, January 1952, N°1, 1-42.
- [6] F. Mayadas, M. Shatzkes, Phyl. Rev. B, Vol.1, N°4, 1382-1389, (1970).
- [7] B. Svenson, Ann. Phys. Vol.25, N°5, (1936).
- [8] Yeong Der Yao, J. H. Tsai, Chinese Journal of Physics , Vol. 16, N°4, 189-195, (1978).
- [9] J.J. Hanak, J. Gitelman, J.P. Pellicane, and S. Bozowski, , J. Appl. Phys., vol. 41, 4958-4962, (1970).
- [10] J.J. Hanak, H. W. Lehmann and R. K. Wehner, J. Appl. Phys., vol. 43, N° 4, 1666-1673, (1972).
- [11] M. Knudsen, Ann. Phys. Leipzig 28, 999, (1909).
- [12] R. J. Gnaedinger, Jr., J. of Vac. Sci. and Technol., 6, N° 3, 355-362, (1969).
- [13] G.C. Schwartz, R. E. Jones, and L.I. Maissel, J. Vac. Sci. and Technol., 6, 351-354, (1969).
- [14] F. M. Smits, Measurement of sheet resistivities with the four point probe, The Bell System technical journal, May 1958, pp.711-717.
- [15] P. Chaudhari: J. of Vac. Sci. and Technol., Vol. 9, N° 1, 520-522, (1971).
- [16] M.K. Loudjani, C. Sella: Int. J. Thin. Fil. Sci. Tec. 4, No. 2, 75-82 (2015).
- [17] Reinder Coehoorn, Novel Magnetoelectronic Materials and devices, Lecture Notes TU/e 2001-2002.